Ordering of Helium Mixtures in Porous Gold

D. J. Tulimieri, J. Yoon,* and M. H. W. Chan
Department of Physics, The Pennsylvania State University, University Park, Pennsylvania 16802
(Received 9 September 1998)

Torsional oscillator measurements show that the phase diagram of ^{3}He-^{4}He mixtures in porous gold is fundamentally different from that of bulk mixtures but similar to that found for mixtures in 98% porous silica aerogel. The similarities found in the mixture phase diagram and in the vapor pressure isotherms in these two media clarify our understanding of the nature of the ordering and the phase transitions in these systems. [S0031-9007(98)08041-7]

PACS numbers: 67.60.–g, 64.70.Fx, 64.70.Ja, 67.40.Kh

It was shown in superfluid decoupling and heat capacity experiments [1,2] that inside aerogel of 98% porosity the ^{3}He-^{4}He mixture phase diagram is completely altered from that of the bulk mixture. As shown in Fig. 1, the well known tricritical point is suppressed, and at high ^{3}He concentration $X_3 = n_3/(n_3 + n_4)$ the phase separation and superfluid transition lines are detached from each other. Here n_3 and n_4 are the numbers of ^{3}He and ^{4}He atoms, respectively. The phase diagram of mixture in aerogel of 95% [3] and 99.5% [4] porosity was found to be topologically the same as that of 98% aerogel. In 87% aerogel, however, it is distinctly different. Three separate experiments using different techniques found only a single superfluid transition phase boundary at high X_3 and the phase boundary originating from low X_3 and low T appears to fade away at intermediate X_3 without attaching to the superfluid transition boundary [5–7]. Recent theoretical [8–10] and experimental [3,7,11] efforts have shed substantial understanding on the mixture in aerogel systems. However, there is as yet no clear microscopic picture of the coexisting phases in the lighter aerogel, and there is no satisfactory explanation of the findings in 87% aerogel.

We have conducted torsional oscillator measurements of helium mixtures in a new medium, porous gold [12], which has a simpler pore geometry than aerogel. In spite of the difference in the pore structure and in the porosity of these two media, we find a phase diagram, also shown in Fig. 1, nearly identical to that in 98% aerogel.

Porous gold is made by selectively leaching silver out of a silver-gold alloy of 70 at. % silver, resulting in a 70% porous structure. Scanning electron micrographs (SEM) show that the substrate consists of interconnected gold strands with a uniform separation between neighboring strands. The diameter of the gold strands, and the characteristic size of the pore structure, can be increased by annealing the sample at a moderate (i.e., well below melting) temperature. The specific surface area of the porous gold sample used in this experiment was determined by methane vapor pressure isotherm (77 K) to be 2.14 m^2/g. Modeling the gold strands as uniform cylinders we find an average strand diameter of 61 nm. Digital image analysis of the SEMs shows a strand and pore size distribution where the width of the distribution at half height is approximately 15% of the pore diameter [12]. Small angle neutron scattering measurement [13] indeed shows a dominant or characteristic length scale in the pore structure of porous gold.

There is no characteristic length in the pore structure of aerogel. Silica aerogel consists of silica strands of about 5 nm in diameter that are interconnected at random sites. The distance between neighboring strands, as deduced by transmission electron micrography [14] and small-angle x-ray scattering measurements, spans a range of 1–100 nm for aerogel of 98.5% porosity [4]. This range is porosity dependent [15]; for aerogel of about 88% porosity it is 1–20 nm. If we use this information to estimate a "pore size" for aerogel, the structure would exhibit a hierarchy of different pore sizes with a maximum pore size that is porosity dependent.

The torsional oscillator used in this study is the same as the one used in recent studies of the superfluid transition of filled pore ^{4}He and ^{4}He films [16]. It has a resonant

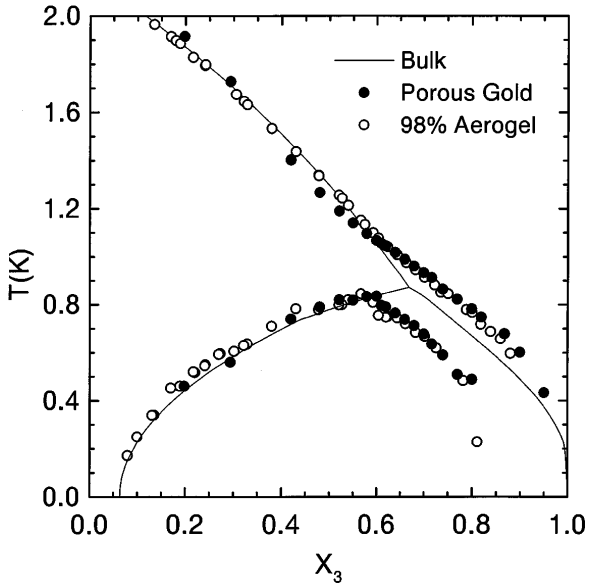

FIG. 1. Phase diagrams of bulk ^{3}He-^{4}He mixtures (solid lines), mixture in 98% aerogel (open circles), and in porous gold (filled circles).

frequency of 578 Hz with a mechanical Q of 6×10^5 at 1 K. The geometric volume of the porous gold sample is 0.04 cm^3 (0.028 cm^3 pore volume) and the torsion bob contains less than 1% bulk space. The resolution of the oscillator is about 6×10^{-6} g/cm^3. It is driven with a constant amplitude ac voltage so that the amplitude of oscillation is inversely proportional to the dissipation in the system.

Starting with pure ^{3}He, the concentration is changed by progressively replacing ^{3}He with ^{4}He while ensuring that that the sample cell remained completely full. This is possible because of the much higher vapor pressure of ^{3}He. Cross calibration showed that X_3 is accurate to $\pm 0.25\%$. The torsional oscillator was mounted to a ^{3}He refrigerator with a base temperature of 350 mK.

In Fig. 2, the decrease in period of the oscillator due to superfluid decoupling, $-\Delta P$, of 14 different mixtures is shown as a function of temperature. Mixtures with $X_3 \geq 0.82$ show a single signature, namely, a sharp decrease in the period corresponding to the superfluid transition at T_c. For concentrations $X_3 < 0.82$, the superfluid decoupling shows hysteretic behavior; i.e., the value of $-\Delta P$ depends on whether data were taken upon warming or cooling, at temperatures well below T_c. In Fig. 3, the amplitude of the oscillator as a function of temperature is shown for eight different mixtures. The smooth curve found for $X_3 = 0.82$ is characteristic of data for $X_3 \geq 0.82$. For $X_3 \leq 0.80$, sharp drops in the amplitude are found upon cooling through a specific temperature T_a. This temperature coincides with the onset of hysteretic behavior in ΔP for mixtures with $0.62 < X_3 < 0.80$. For $X_3 < 0.62$, onset of hysteresis in ΔP is found to commence below T_a by 50 to 100 mK. Following Refs. [1,3], we interpret the sharp decrease in the amplitude as a signature of the phase separation of the system. This decrease in amplitude (i.e., increase in dissipation) is likely related to the sudden increase in interfaces related to phase separation. The phase diagram shown in Fig. 1 is the compilation of T_c and T_a for mixtures of 22 different X_3.

We propose below a microscopic model of the different phases depicted in Fig. 1 for porous gold and show how this model is also applicable to mixtures in aerogel. The initial 1%–2% of ^{4}He added to the ^{3}He is preferentially adsorbed on the surface as a bound solid layer. With increasing ^{4}He, a ^{4}He-rich superfluid film develops on the gold surface while the interior of the pore is filled with nearly pure ^{3}He. As X_3 decreases, the ^{4}He-rich film thickens causing an increase in superfluid decoupling and in the transition temperature T_c. If we assume that the concentration of ^{3}He in the superfluid film is bulklike (i.e., 6.4% ^{3}He at $T = 0$) and the ^{3}He-rich interior is completely free of ^{4}He, then the thickness of the ^{4}He-rich film in the $T = 0$ limit is approximately 4.5 nm at the coexistence boundary ($X_3 \approx 0.85$). We refer to this configuration, where the entire surface is covered by a ^{4}He-rich film, as the film phase.

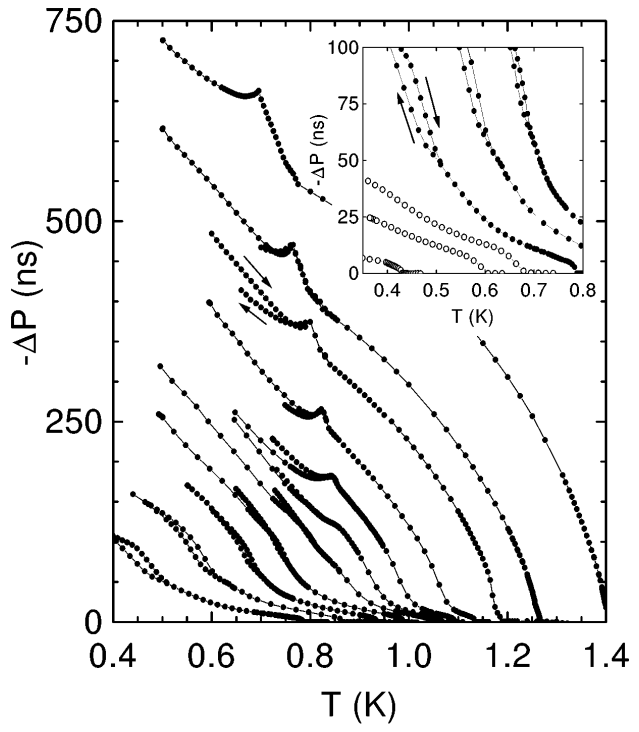

FIG. 2. The period change $-\Delta P$ of the oscillator versus T for 14 different mixtures. X_3 of these mixtures in the main figure, in increasing order of T_c, are 0.800, 0.740, 0.700, 0.660, 0.620, 0.600, 0.579, 0.550, 0.521, 0.480, and 0.420. For clarity, data for $X_3 = 0.950$, 0.900, 0.868, 0.800, 0.740, and 0.700 are shown in the inset. $-\Delta P$ shows history dependent behavior at low temperature only for $X_3 < 0.82$. The arrows on two of the mixtures indicate data taken while warming or cooling.

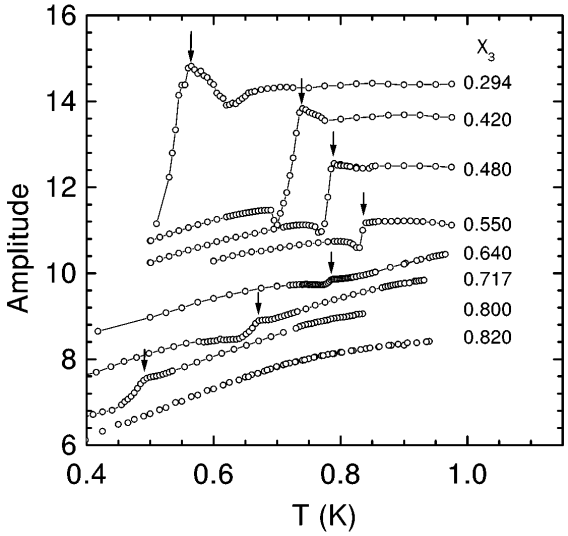

FIG. 3. The amplitudes of the torsional oscillator (with constant drive voltage) in arbitrary units vs T for eight different mixtures. Except for $X_3 = 0.82$, the amplitudes show a drop upon cooling through a specific temperature T_a, the temperature of phase separation. T_a are marked by arrows.

Further addition of ^{4}He does not cause film thickening, but causes filling of some pores with the same ^{4}He-rich solution which comprises the superfluid film. This state we refer to as the "filled" phase. Thus, the coexistence region consists of a phase containing a ^{4}He-rich film on the substrate, with the interior of the pore filled with a ^{3}He "bubble," and a phase in which the ^{4}He-rich solution fills the pore, bridging the gap between neighboring gold strands. This is analogous to capillary condensation in a liquid-vapor system with the ^{3}He-rich phase corresponding to the vapor phase. As X_3 is reduced, the radius of curvature of the ^{3}He bubbles remains unchanged, but the portion of the interior region occupied by these bubbles is reduced, giving way to the filled pore phase. When the film phase is completely replaced by the filled pore phase, the system emerges from the coexistence region into the miscible ^{4}He-rich superfluid region of the phase diagram.

As shown in Fig. 1, the coexistence region of the film and filled phase is found to extend to higher temperature at intermediate concentrations, terminating at a ^{3}He-^{4}He critical point. The shape of the coexistence boundary resembles that of the bulk, i.e., mixture free of porous medium, liquid-vapor, and binary fluid systems. In the miscible phase, outside of the coexistence region, a concentration gradient exists as a function of distance from the gold strands but does so without any sharp boundary [4].

The coexistence of an adsorbed liquid film with capillary condensed (filled) pores in porous gold is also seen in a vapor pressure adsorption isotherm study performed at 2.18 K (Fig. 4a). This isotherm was carried out on the sample used in this study before the pores were enlarged by annealing [16]. The characteristic pore size was about 30% smaller at that time. For small amounts of adsorbed helium a film forms on the surface throughout the sample. After the first 2–3 monolayers the equilibrium vapor pressure increases rapidly with continued adsorption. When the vapor pressure reaches $P/P_0 = 0.982$ (P_0 is the saturated vapor pressure), adsorbing more helium does not increase the film thickness uniformly. Instead, the surface tension causes capillary condensation in some regions of the sample, filling the space between neighboring gold strands completely with liquid helium. The entire condensation event occurs over a vapor pressure range of less than two parts in 10^3. Since vapor pressure determines the chemical potential, the constancy in P supports our interpretation that the capillary condensation event shown here corresponds to the coexistence of a film phase with vapor bubbles of a constant radius of curvature and the filled pore phase. This finding in the liquid-vapor system suggests that in the mixture system the radius of curvature of ^{3}He bubbles in the film phase at a fixed temperature also remains constant throughout the coexistence region. Liu *et al.* [17] performed a simulation of binary fluid mixtures in a cylindrical pore and observed the same behavior. The coexistence region described above corresponds to the "capsule" phase of Ref. [17].

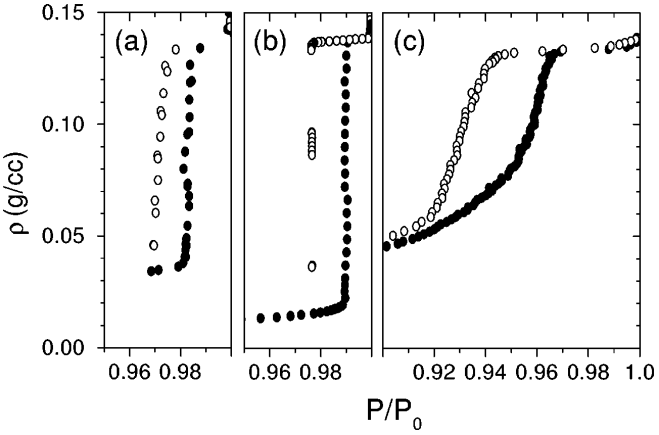

FIG. 4. ^{4}He vapor pressure isotherm near the saturated vapor pressure P_0 of ^{4}He in porous gold at $T = 2.18$ K (a), in 98% aerogel at 2.34 K (b), and in 87% aerogel at 2.42 K (c). The vertical scale shows amount of helium adsorbed per cm^3 of pore volume. Filled and open symbols show data taken during filling and draining processes of the isotherm, respectively.

A very sharp capillary condensation event, as shown in Fig. 4b, is also seen in the adsorption of ^{4}He in 98% aerogel. This is unexpected, considering the complicated pore structure of aerogel. It appears that capillary condensation occurs in two regimes in this case. In the low coverage regime, capillary condensation occurs in the smallest crevices defined by neighboring silica strands which have the greatest tendency to fill. As pressure and ^{4}He coverage is increased, progressively larger crevices are filled. This is a regime of "gradual" capillary condensation. We speculate that in light aerogels of porosities larger than 95%, this process continues until all of the small structure is covered, leaving a liquid-vapor interface with a well defined and uniform concave radius of curvature throughout the sample. The curvature is determined by the vapor pressure and the largest separation between strands in a given sample. Further adsorption reduces this radius of curvature until it reaches the stability limit and the isotherm ends with a "major" capillary condensation event at $P/P_0 = 0.990$. As in the case of porous gold, the extremely narrow vapor pressure range of the event (less than one part in 10^3 in this case) supports the interpretation that the condensation corresponds to the coexistence of the film and filled phases.

In the case of ^{3}He-^{4}He mixtures, gradual capillary condensation of ^{4}He rich solution into the small crevices of 98% aerogel takes place as X_3 is reduced from 1 to about 0.85, the coexistence boundary at $T = 0$. The coexistence region corresponds to the major capillary condensation event, where the film phase with ^{3}He bubbles of a constant radius of curvature (defined by the largest separation between the silica strands) is replaced by the filled (with ^{4}He solution) phase as X_3 is reduced

from 0.85 to about 0.065. Since the largest separation between the silica strands in 98% aerogel, about 100 nm, is comparable to the characteristic pore size in porous gold, the similarity in the diagram of the two systems is not surprising.

The vapor pressure isotherm in 87% aerogel, shown in Fig. 4c, on the other hand, does not show a major capillary condensation event. When 87% aerogel is partially filled, all of the crevices surrounded by neighboring silica strands smaller than a given size are filled with liquid helium, while the larger crevices have vapor bubbles. Since the largest separation between silica strands is only on the order of 20 nm the process of gradual capillary condensation continues until the aerogel is completely filled with liquid ^{4}He without entering into a well defined film phase as in 98% aerogel. As a consequence, there is no two phase coexistence or major capillary condensation event.

The absence of a two phase coexistence in the liquid-vapor system makes plausible the absence of the coexistence of film and filled-pore phases of the mixture in 87% aerogel. As X_3 is reduced from 1, the silica surface is first coated with a solid layer of pure or nearly pure ^{4}He. Continued decrease in X_3 thickens the ^{4}He-rich film and induces capillary condensation of ^{4}He-rich solution between the silica strands, progressing into space of increasing separation. This process leads to a system that supports superfluidity at progressively higher temperatures. The single phase boundary found in 87% aerogel at high X_3 is indeed consistent with a superfluid transition and not related to phase separation [5–7]. This boundary also connects smoothly to the superfluid transition boundary at low X_3 [5–7]. These findings are not consistent with the interpretation of a bulklike phase diagram with a tricritical point for ^{3}He-^{4}He mixtures in 87% aerogel [7]. Since the ^{3}He-rich solution must be accommodated inside the aerogel sample, ^{3}He-rich bubbles are found even in mixtures of low X_3. (This is in contrast to the liquid-vapor system.) The bubbles finally disappear when the mixture is completely miscible. This disappearance of the ^{3}He bubbles is marked by the phase boundary seen at low X_3 and low T [5–7]. The phase diagram of mixtures in 87% aerogel (in contrast to that in 98% aerogel and porous gold) indicate that finite solubility of ^{3}He in ^{4}He at low T is a necessary but not sufficient condition for film-filled phase coexistence.

In summary, torsional oscillator measurements of ^{3}He-^{4}He mixtures in porous gold show that the phase diagram is very similar to that of mixtures in 98% aerogel. With the aid of vapor-pressure isotherm results, we arrive at a model where the coexisting phases are a ^{4}He-rich film phase enclosing ^{3}He-rich bubbles of a constant radius of curvature that depends on T, but not on X_3, and a filled phase where the pore space between the strands is capillary condensed with ^{4}He-rich solution. While our model of the ordering of helium mixtures in aerogel and in porous gold seems reasonable and consistent with available thermodynamic information, direct structural confirmation via, for example, small-angle x-ray scattering studies of the system is clearly desirable.

We acknowledge informative discussions with Jayanth Banavar, Nihat Berker, Milton Cole, Andrea Liu, Jonathan Machta, Norbert Mulders, and Mark Paetkau. The work reported here is supported by NSF under Grant No. DMR-9630736.

*Present address: Department of Electrical Engineering, Princeton University, Princeton, NJ 08544.

[1] S. B. Kim, J. Ma, and M. H. W. Chan, Phys. Rev. Lett. **71**, 2268 (1993).
[2] N. Mulders and M. H. W. Chan, Phys. Rev. Lett. **75**, 3705 (1995).
[3] J. Yoon, N. Mulders, and M. H. W. Chan, J. Low Temp. Phys. **110**, 585 (1998).
[4] M. H. W. Chan, N. Mulders, and J. Reppy, Phys. Today **49**, No. 8, 30 (1996).
[5] J. Yoon *et al.*, Czech. J. Phys. **46**, Suppl. S1, 157 (1996).
[6] D. J. Tulimieri, N. Mulders, and M. H. W. Chan, Czech. J. Phys. **46**, Suppl. S1, 199 (1996).
[7] M. Paetkau and J. R. Beamish, Phys. Rev. Lett. **80**, 5591 (1998).
[8] L. Pricaupenko and J. Treiner, Phys. Rev. Lett. **74**, 430 (1995).
[9] A. Falicov and A. N. Berker, Phys. Rev. Lett. **74**, 426 (1995).
[10] A. Maritan *et al.*, Phys. Rev. Lett. **67**, 1821 (1991).
[11] A. Golov, J. V. Porto, and J. M. Parpia, J. Low Temp. Phys. **110**, 591 (1998); N. Kalechovsky and D. Candela, J. Low Temp. Phys. **101**, 379 (1995); D. Candela and N. Kalechofsky, J. Low Temp. Phys. **113**, 351 (1998).
[12] R. Li and K. Sieradzki, Phys. Rev. Lett. **68**, 1168 (1992).
[13] R. C. Newnam and K. Sieradzki, Science **263**, 1708 (1994).
[14] G. C. Ruben, L. W. Hrubesh, and T. M. Tillotson, J. Non-Cryst. Solids **186**, 209 (1995).
[15] A. Boukenter *et al.*, J. Phys. (Paris) Colloq. **50**, C4-133 (1989); P. A. Crowell *et al.*, Phys. Rev. B **51**, 12 721 (1995).
[16] J. Yoon and M. H. W. Chan, Phys. Rev. Lett. **78**, 4801 (1997); G. A. Csáthy *et al.*, Phys. Rev. Lett. **80**, 4482 (1998).
[17] A. J. Liu *et al.*, Phys. Rev. Lett. **65**, 1897 (1990).